Segmentation and 3D visualization of high-resolution human brain cryosections

Ikuko Takanashi[1], Eric Lum[1], Kwan-Liu Ma[1], Joerg Meyer[2], Bernd Hamann[1], Arthur J. Olson[3]

[1]Center for Image Processing and Integrated Computing & Department of Computer Science, University of California, One Shields Avenue, Davis, CA 95616-8562, USA

[2]Computer Science Department, Mississippi State University, Mississippi State, MS 39762, USA

[3]The Scripps Research Institute, 10550 North Torrey Pines Road, La Jolla, CA 92037, USA

ABSTRACT

We present a semi-automatic technique for segmenting a large cryo-sliced human brain data set that contains 753 high-resolution RGB color images. This human brain data set presents a number of unique challenges to segmentation and visualization due to its size (over 7 GB) as well as the fact that each image not only shows the current slice of the brain but also unsliced "deeper layers" of the brain. These challenges are not present in traditional MRI and CT data sets. We have found that segmenting this data set can be made easier by using the YIQ color model and morphology. We have used a hardware-assisted interactive volume renderer to evaluate our segmentation results.

Keywords: Color models, cryosections, morphological operations, medical imaging, segmentation, volume rendering

1. INTRODUCTION

Modern medical imaging technology is capable of generating huge amount of volumetric data for routine clinical studies. As data sets become larger in resolution and overall size, it becomes impractical to segment exclusively by hand. Real-color RGB images, such as cryosections, generally contain much more information than CT or MRI data. The resolution of each individual image (150-500 dpi) is very high, and the color information provides additional cues. A typical cryosection volume data set can be several orders of magnitude larger than CT or MRI volume data. For example, the Visible Human data set consists of color cryosections of the whole bodies of a male and a female, with each section at a resolution of 2048×1216 pixels.

We have developed a semi-automated segmentation pipeline, which allows us to apply different filters and image processing algorithms to separate the tissue from the surrounding material for typical cryosection data. This semi-automated segmentation capability can significantly cut down the time to perform high-resolution volumetric image analysis.

2. HUMAN BRAIN DATA SET

The human brain data set we have used (courtesy of Art Toga, Laboratory of Neuro Imaging, UCLA) has a resolution of 1472x1152 pixels and consists of 753 cryosections of a frozen human brain. [1,2] The data set provides real-color RGB information, 16 bits per channel, and the size of each image is about 10 MB. The cryoslice process used to create this data set consisted of taking photographs of the human brain after removing successive thin slices from the top to the bottom. For this data set, the slices were so thin that scanning was virtually impossible. Instead, photos were taken of the unsliced portion of the brain rather than the removed slice itself. A number of unique segmentation challenges arise not encountered with MRI or CT data since each image can contain data that is part of deeper layers. In particular, cavities or gaps in the brain reveal structures that are actually located in deeper layers, as illustrated in Figure 1. The cryosections of the Visible Human data set do not exhibit this problem since the cavities were filled with blue latex to block projection of deeper structures onto the image plane.

To correctly segment the UCLA brain data, the parts of the image corresponding to cavities need to be eliminated and replaced by a transparent region. The brain must also be separated from the surrounding matter, i.e., from the ice and the background (see Figure 2 (a)).

Corresponding author: Kwan-Liu Ma; e-mail addresses: ikuko@ucdavis.edu, {lume,ma,hamann}@cs.ucdavis.edu, jmeyer@cs.msstate.edu, olson@scripps.edu.

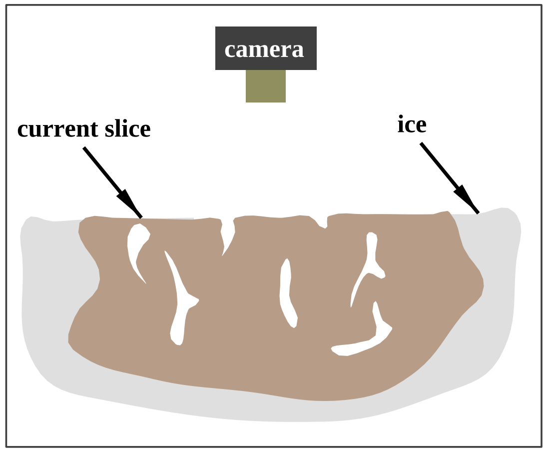

Figure 1: Picture of current slice also reveals materials in deeper layers due to cavities and gaps.

3. SEGMENTATION

3.1. Exploring Color Cues

A great deal of research has been done in segmentation of CT and MRI data sets,[3,4] usually to identify specific organs. Unlike MRI and CT data, which is grayscale, cryo-sliced data contains color information of which segmentation processes may make use. Color offers a number of visual cues that can be used to distinguish features in the data set. The brain can be distinguished from the ice and the background relatively easily by using color information. However, it is difficult to distinguish between a current layer of the brain and deeper layers of similar brain material.

After studying the cryo-sliced images of the brain, we have found that red and light brown components are more dominant in the current layer of the brain than the deeper layers. We have conducted experiments with a number of different colorspaces,[5] including RGB, HLS, HSV, grayscale, and YIQ in an attempt to find one that would make brain-colored material more visible than its surroundings. HSV works reasonably well, but cannot segment darker brown regions in a current layer of the brain. We found that the YIQ color model works best for selecting the brownish colors of the brain; in particular, the I component includes color components from orange to cyan. We have applied this formula to convert from RGB to YIQ color space:

$$\begin{bmatrix} Y \\ I \\ Q \end{bmatrix} = \begin{bmatrix} 0.299 & 0.587 & 0.114 \\ 0.596 & -0.275 & -0.321 \\ 0.212 & -0.523 & 0.311 \end{bmatrix} \begin{bmatrix} R \\ G \\ B \end{bmatrix}$$

Dai and Nakano[6] use the I component of the YIQ color model to extract facial regions from images. The fact that the same model works for the brain can probably be explained by the skin-like color of the brain. The HSV color model has also been used to extract facial regions from images.[7] The I component of YIQ contains in-phase modulation. The smaller the value of the I component, the more it contains orange hues and the less it contains cyan hues. Dai and Nakano use I values in the range of 0 to 0.20 to extract skin-colored regions. For the human brain data set, we use I values from 0.069 to 0.084. Figure 2(b) shows the resulting image for slice 550. The brain is segmented reasonably well. However, the image still shows holes inside the brain and some noise around the brain. To fill these holes, to smooth the contour and to remove the surrounding noise, we apply filtering techniques after YIQ thresholding.

3.2. Filtering

Color thresholding applied alone results in very noisy images. This noise consists of salt-and-pepper in regions that have a color near the threshold. In addition, there is noise due to the physical cutting process, and thresholding results in holes since some pixels of the current layer can have the same dark color as those regions in a deeper layer. To minimize these problems a series of filtering steps is performed. The slices are filtered one-by-one, layer-by-layer. Since the size of the data set is over 7 GB, we deal with individual slices instead of the entire volume. Results of the filtering process are shown in Figures 2(c)-(f). Some steps clean up noise in one area but add new noise in the process, which is removed later. The segmentation pipeline consists of the following steps:

(1) Median filter Thresholding of the I component works reasonably well for selecting pixels in the brain volume. However, it also incorrectly selects some pixels because deeper layers of the brain can have a light brown color, and there are some brain-colored pixels that result from small brain debris created in the slicing process. The brain can be divided into white- and gray-matter regions, with the white matter being a brighter brown than the gray-matter. [8] Some images of the brain have very dark brown gray-matter pixels that are not selected since their I component is too low (similar to that of a pixel belonging to a deeper layer). To fill these small holes and remove salt-and-pepper noise we apply a median filter after color thresholding. The window size of the filter is 5x5 pixels. Figure 2(c) shows the result of applying the median filter to slice 550.

(2) Region Size Thresholding During the physical cutting process, small pieces of the brain were removed and deposited in areas around the brain. These pieces appear in some of the cryo-sliced images as small areas of brain-colored noise (Figure 3(a)). In addition, some areas of the deeper layers are light brown and not removed by color thresholding. To remove this noise, we apply a region growing algorithm to find regions that are small enough to be classified as noise. Due to the cryo-slicing process, specific areas have different-size debris. We have used six different thresholds for the size of the artifacts in the 753 images. Figure 2(d) shows an image of slice 550 after region size thresholding, and Figures 3(a) and 3(b) show the original image of slice 450 and the result after region size thresholding, respectively.

(3) Morphological operations To fill the gaps inside the brain and smooth the contour, we apply morphological operations. We use a 9x9 circular structuring element and apply dilation to each image. This process fills in small noisy gaps in the brain that were not filled in by the median filter process. It is important that this step be performed after median filtering and region size thresholding, since dilation could make small noise outside the brain become even larger. Dilation also makes the edges of the brain smoother. However, iced areas around the brain are also added (Figure 2(e)).

(4) RGB thresholding To remove iced areas added in the previous step, we apply thresholding in the RGB color space. Extra weight is put on the blue component, since blue is not very prevalent in the brain (Figure 2(f)).

For some steps, we must use several threshold values since the structure of the brain typically changes across the data set. For example, three different values were used for YIQ and seven for region size. However, it is much easier to select a set of thresholds than to segment the entire data set by hand.

4. VOLUME RENDERING

The segmented images are volume-rendered in hardware using three sets of 2D textures, [9] with each set aligned to one of the data set's principal axes. Each texture contains RGBA color components, where the alpha value is used to vary the opacity of the brain, or to make transparent those areas of the data set that were removed in the segmentation process.

With an AMD 1.2 GHz Athlon processor with 768MB of main memory and a 64MB Nvidia GeForce 3 video card, a downsampled 256^3 volume with 32-bits per voxel can be rendered at about 10fps. By using 16-bit textures, the amount of video memory utilized is reduced in half, allowing larger volumes to be visualized at higher frame rates at the expense of color accuracy.

An interface has been created that allows a user to interactively rotate the brain volume (Figure 4(a)). A user can also apply multiple axis-aligned cutting planes to quickly visualize specific regions of the brain (Figure 4(b)). For example, the gaps and cavities of the brain are visible (Figure 4(c),(d)). In addition, the opacity map can be varied based on voxel intensity to emphasize either the white- or gray-matter regions.

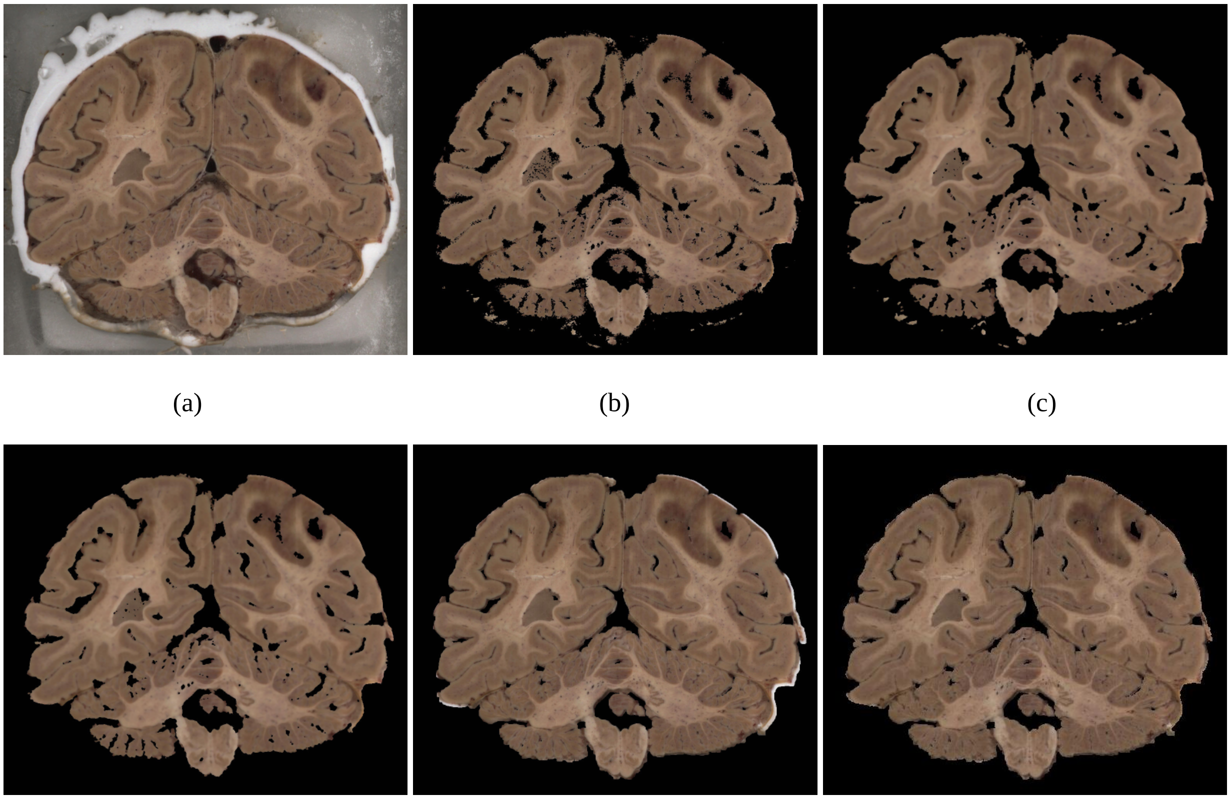

(a) (b) (c)

(d) (e) (f)

Figure 2. Slice 550: (a) Original, (b) YIQ thresholding, (c) median filter, (d) region size thresholding, (e) morphology (dilation), and (f) RGB thresholding.

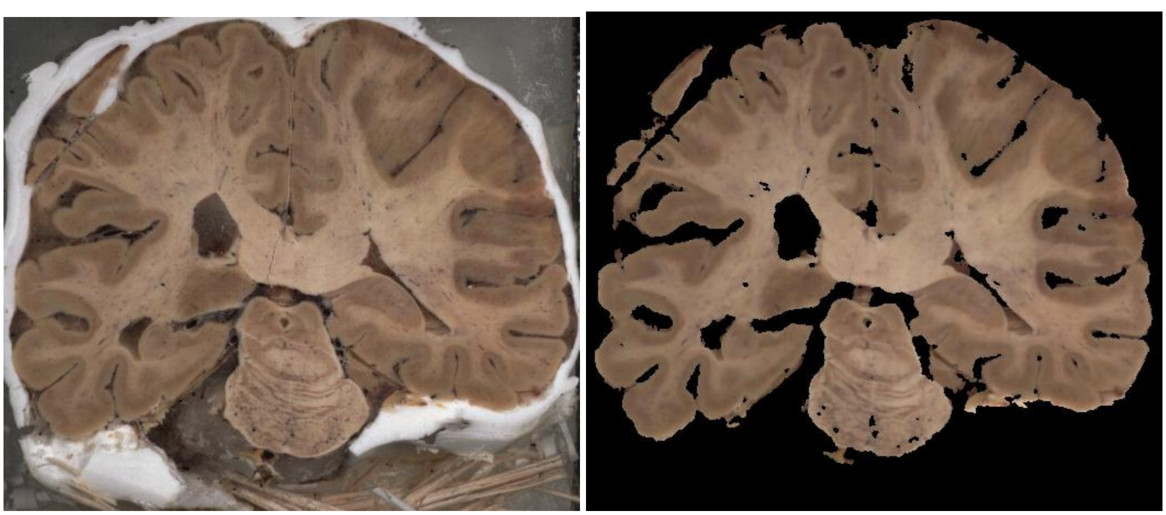

(a) (b)

Figure 3: Slice 450: (a) Original image and (b) region size thresholding.

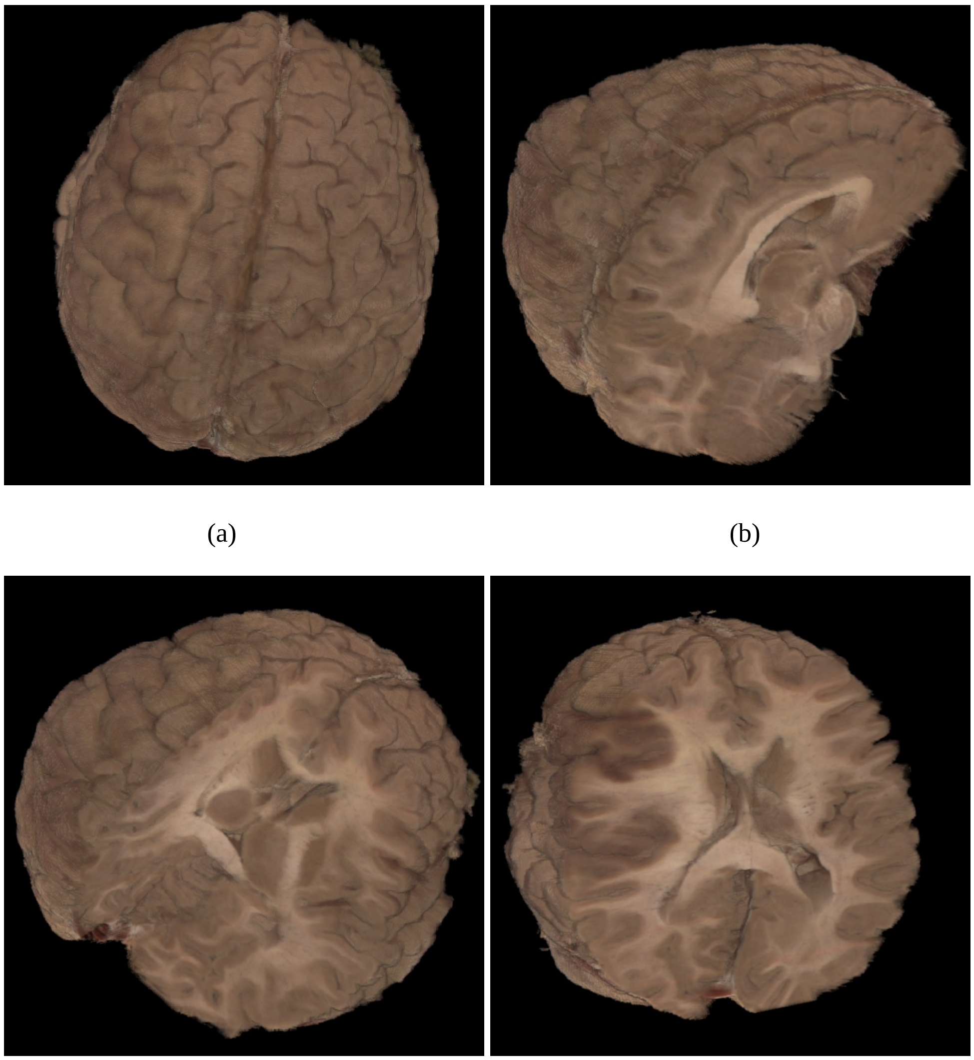

(a) (b)

(c) (d)

Figure 4: Volume rendering of segmented data: (a) back view, (b) side removed, (c) and (d) showing gaps and cavities.

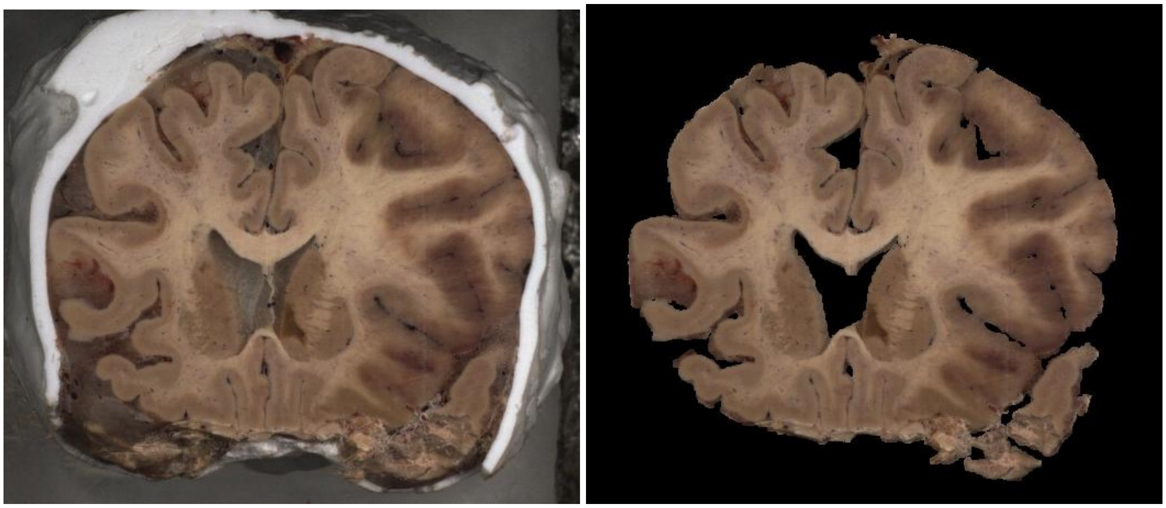

(a) (b)

Figure 5: Slice 250: (a) Original image and (b) segmented image.

5. DISCUSSION AND FUTURE WORK

We have obtained good results for most slices. However, depending on the part of the brain, we have encountered several difficulties. For example, in the segmented result (Figure 5(b)) for slice 250 (Figure 5(a)), the darker areas (upper-right part) are removed, but this area should remain as a part of the current layer. Also, some noise (upper-middle part) in the deeper layer has not been removed because we are using only one I component threshold value for each slice. If multiple parameter values were used for each slice depending on the features present in the slice, better results could be obtained. However, setting the parameter values can be a difficult and time-consuming process. Adding more parameters also makes the process more complex. To find the values of these parameters more easily it is helpful to have an interactive volumetric user interface to select regions and change parameter values. Furthermore, an automated mechanism to find these values would be beneficial. To set the parameter values, it is necessary to know which areas should be removed and retained. Although we have discussed this with some physicians, more knowledge of the topology of the brain could be incorporated in the algorithm to obtain better results.

6. CONCLUSIONS

We have successfully segmented a high-resolution human brain cryoslice data set. This human brain data presented a number of challenges due to the size of the data set and the fact that each image not only shows the current slice of the brain but also unsliced deeper layers. We have removed the ice and tray surrounding the brain as well as deeper layers of the brain from each image. The deeper layers exist not only around a current layer but are also visible through cavities and gaps. We have successfully segmented those areas. We believe our approach could be applied to other large cryosection data sets, perhaps to classify different tissues of an organ. For example, we can apply our method to segment the white- and gray-matter of a human brain data set.

Interactive volume rendering allows us to visualize the human brain in three dimensions and explore both shape and color of the brain from arbitrary viewpoints. A user can change the opacity map based on voxel intensity to emphasize the white- or gray-matter regions. Specific regions can also be seen using interactive volume cutting such that the detection of cavities or gaps can be verified.

ACKNOWLEDGMENTS

This work was supported by NSF (CAREER Awards: ACI 9624034, ACI 9983641; LSSDSV: ACI 9982251; and NPACI) and the Office of Naval Research (ONR, N00014-97-1-0222). Funding was also provided by the Center for Neuroscience, UC Davis, under contract NIMH 2 P20 MH60975-06A2 (National Institute of Mental Health and National Science Foundation). Dr. Arthur Toga at the Laboratory of Neuro Imaging, UCLA, kindly provided the data set.

REFERENCES

1. A. Toga, K. Amback, B. Quinn, M. Hutchin, and J. Burton, "Postmortem anatomy from cryosectioned whole human brain," *J Neurosci Methods* **54**(2), pp. 239–252, 1994.
2. A. Toga, K. Ambach, and S. Schluender, "High-resolution anatomy from in situ human brain," *NeuroImage* **1**, pp. 334–344, 1994.
3. M. Bomans, K. H. Höhne, U. Tiede, and M. Riemer, "Three-dimensional segmentation of mr images of the head for 3d display," *IEEE Transactions on Medical Imaging* **9**(3), pp. 177–183, 1990.
4. S. P. Raya, "Low-level segmentation of 3d mr brain images - a rule based system," *IEEE Transactions on Medical Imaging* **9**(3), pp. 327–337, 1990.
5. R. Gonzalez and R. Woods, *Digital Image Processing*, Addison-Wesley, 1992.
6. Y. Dai and Y. Nakano, "Face-texture model-based on sgld and its application in face detection in a color scene," *Pattern Recognition* **29**, pp. 1007–1017, June 1996.
7. K. Sobottka and I. Pitas, "Extraction of facial regions and features using color and shape information," in *Proceedings of the International Conference Of Pattern Recognition (ICPR '96)*, pp. 421–425, August 1996.
8. J. Nolte, *The Human Brain, An Introduction to Its Functional Anatomy*, Mosby, fourth ed., 1999.
9. C. Rezk-Salama, K. Engel, M. Bauer, G. Greiner, and T. Ertl, "Interactive volume rendering on standard PC graphics hardware using multi-textures and multistage rasterization," *Eurographics/SIGGRAPH Workshop on Graphics Hardware 2000* , pp. 109–118, 2000.